Received 21 November 2020; accepted 29 December 2020. Date of publication 1 January 2021; date of current version 28 January 2021.
The review of this article was arranged by Editor C. Surya.

Digital Object Identifier 10.1109/JEDS.2020.3048725

Exceptionally Linear and Highly Sensitive Photo-Induced Unipolar Inverter Device

MUHAMMAD NAQI [1], JI YE LEE [2], BYEONG HYEON LEE [3,4], SUNKOOK KIM [1], SANG YEOL LEE [5], AND HOCHEON YOO [5]

1 Department of Advanced Materials Science and Engineering, Sungkyunkwan University, Suwon 16419, South Korea
2 Department of Semiconductor Engineering, Cheongju University, Cheongju 28503, South Korea
3 Korea University, Seoul 136-701, South Korea
4 Research Institute of Advanced Semiconductor Convergence Technology, Chongju 28503, North Korea
5 Department of Electronic Engineering, Gachon University, Seongnam 13120, South Korea

CORRESPONDING AUTHORS: S. Y. LEE AND H. YOO. (e-mail: sylee2020@gachon.ac.kr; hyoo@gachon.ac.kr)

This work was supported in part by the National Research Foundation of Korea under Grant NRF-2018R1A2B2003558; in part by the Basic Science Research Program through the National Research Foundation of Korea (NRF) funded by the Ministry of Education under Grant NRF 2017R1D1A3B06033837; in part by the Korea Institute of Energy Technology Evaluation and Planning (KETEP); in part by the Ministry of Trade, Industry and Energy (MOTIE) of the Republic of Korea under Grant 20172010104940; and in part by the MSIT (Ministry of Science and ICT), Korea, under the Grand Information Technology Research Center Support Program under Grant IITP-2020-0-01462 supervised by the IITP (Institute for Information & Communications Technology Planning & Evaluation). The work of Hocheon Yoo was supported by the National Research Foundation of Korea Grant funded by the Korea Government (MSIT) under Grant NRF-2020M3A9E4104385 and Grant NRF-2020R1A2C1101647. *(Muhammad Naqi and Ji Ye Lee contributed equally to this work.)*

ABSTRACT Oxide semiconductors are of particular interest in the field of integrated electronics due to their large-area fabrication, high uniformity, and superior performance. Here, we report an exceptionally sensitive photo-induced inverter device with high linearity based on the unipolar n-type channel material amorphous silicon indium zinc oxide (a-SIZO). The field-effect transistor (FET) based on a-SIZO exhibits maximum mobility of 9.8 cm^2/Vs at V_D of 5 V, high on/off ratio of $\sim 10^6$, and stable threshold voltage (V_{Th}) of −0.35 V. Additionally, the optical properties of the proposed FET include excellent V_{Th} shift and photocurrent (I_{photo}) with high linearity under various red-light illumination. The proposed enhancement-load type inverter device shows reliable electrical and optical characteristics with an inverter gain of 0.7 at V_{DD} of 1 V and linear photo-response in terms of inverter gain and voltage shift, demonstrating promising potential in the field of integrated electronics for optoelectronic applications.

INDEX TERMS Unipolar inverter, amorphous silicon indium zinc oxide (a-SIZO), field-effect transistor (FET), phototransistor, photo-induced inverter.

I. INTRODUCTION

Oxide semiconductors have gained tremendous attention in the field of integrated electronics due to their high-electrical performance, large-area fabrication, and simple processing techniques [1], [2]. Recently, the use of various organic and oxide semiconductor material systems for p- and n-type material in high-electrical performance complementary metal-oxide-semiconductor devices have been reported but limited by the complex structure and costly and complicated processing techniques [3], [4]. To overcome this issue, unipolar integrated circuits (ICs) have been reported to achieve greater electrical performance and high integration using only n- or p-type semiconductor material, having relatively simple structure and processing methods [5], [6]. Previously, oxide semiconductor material systems gained much attention in the electronic and optoelectronic field due to their wide bandgap (>3.2 eV) and superior carrier transport properties despite their amorphous structure and low-temperature processing requirements [2], [7]–[9]. Among the various types of photo-sensitive devices, amorphous oxide semiconductors (AOSs) are exceptionally promising channel materials due to their visible spectral wavelength detectivity and intensity-selectivity of incident light [9], [10]. Despite their integration in high-performance FET devices, much effort is still required to investigate the properties of AOS-based

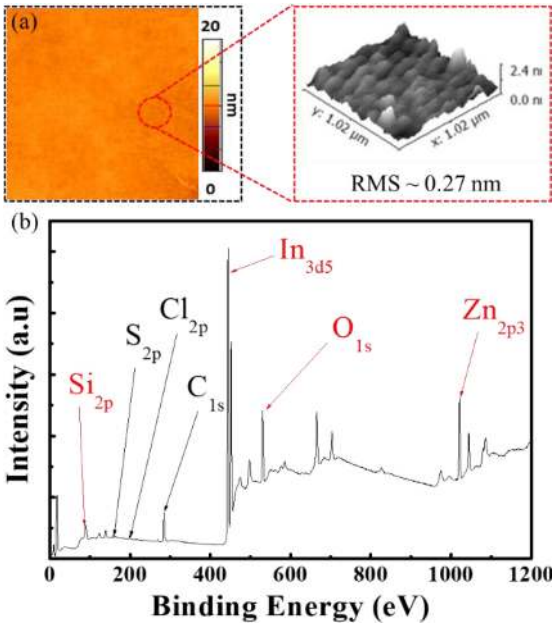

FIGURE 1. (a) Surface roughness analysis of deposited a-SIZO film using the atomic force microscope (AFM) method. (b) Material characterization of a-SIZO film through x-ray photoelectron spectroscopy (XPS) analysis.

devices for next-generation ICs and optoelectronic applications.

Herein, we have introduced a photo-induced inverter device based on amorphous silicon indium zinc oxide (a-SIZO) channel material, exhibiting high-performance electrical and optical properties with highly linear photosensitivity and inverting properties with respect to the incident light power. In this study, an enhancement-load type inverter device has been fabricated using a conventional lithography process. The proposed a-SIZO based field-effect transistor (FET) exhibits high electrical performance with maximum mobility of 9.8 cm^2/Vs, on/off current ratio of 1×10^6, and a stable threshold voltage of -0.35 V. Optical properties of presented a-SIZO based FET are also measured, revealing stable and linear results in terms of photocurrent (I_{photo}), threshold shift (ΔV_{Th}), and rapid time response. The presented design of a unipolar inverter device exhibits high inverting electrical properties over a small voltage range (V_{DD}; 0.2 V $\sim$ 1.0 V) and maximum inverter gain of 0.7. Additionally, the optical measurements of the proposed inverter have also been analyzed under red-light illumination wavelength of 638 nm, exhibiting high linearity, and stable photo-responsive behavior. Although the proposed a-SIZO based photo-induced inverter presented in this article was initially intended to enable excellent optical measurements in integrated electronic circuits, we believe that the present work may provide a new platform to combine IC and optoelectronics for futuristic applications.

II. EXPERIMENTAL

To fabricate the proposed photo-induced inverter device, firstly, the gate electrode was patterned onto the cleaned rigid glass by using the photolithography process. To pattern the gate electrodes, the etching method was utilized in which the photoresist (PR-AZGXR-601, MERCK) was spin-coated onto the titanium/gold (Ti/Au, the thickness of 10/50 nm) deposited rigid glass substrate at 3000 rpm for 20 s and then exposed to a UV light for 1.5 s in presence of patterned mask. Then, the pattern was developed in a developer solution (AZ-300MIF) for 20 s and followed by the annealing process for 15 min at 120 °C. The unwanted area of Ti/Au was then removed by putting the developed sample in Au etchant and buffer oxide etchant (BOE) for 10 s and 20 s, respectively. After patterning the gate electrode, the dielectric layer of Al_2O_3 (80 nm) was deposited using atomic layer deposition (ALD) method at 200 °C. To etch the unwanted area of the deposited Al_2O_3 layer, the abovementioned photolithography was used. The a-SIZO channel material was deposited by radio frequency (RF) magnetron sputtering at room temperature (sputtering power of 30 W, the deposition rate of 2 mTorr, and Ar: O_2 flow ratio of 30:0) onto the Al_2O_3 surface and then patterned by the etching process, mentioned above. Finally, the source and drain electrodes were patterned by using the lift-off process after annealing the a-SIZO patterned sample at 150 °C for 2 hours in ambient conditions. The channel length and width were defined as 20 and 100 μm, respectively. Also, the source and drain electrodes were patterned in a way to connect the gate and drain of load FET to obtain the enhancement-load type inverter device. The electrical measurements of FET and inverter devices were measured using a semiconductor characterization system (Keithley, 4200 SCS). Optical characteristics were observed under red light illumination wavelength of 638 nm (Thorlabs, SM600) at ambient conditions.

III. RESULTS AND DISCUSSION

The material properties of deposited a-SIZO were characterized in terms of x-ray photoelectron spectroscopy (XPS), atomic force microscopes (AFM) morphology, and Transmission electron microscopy (TEM) at ambient conditions. Figure 1a shows the surface roughness image of the a-SIZO film using the AFM method. The root means square (RMS) roughness of 0.27 nm was obtained during experiments, elaborating a smooth surface of a-SIZO channel material which is useful for compressing scattering centers and interface traps. Reference [11] The existence of the related elements (silicon (Si), indium (In), zinc (Zn), and oxygen (O)) was confirmed by the XPS analysis, as shown in Figure 1b. In addition, the 23 nm thickness of the proposed a-SIZO channel material was confirmed by the TEM method, shown as a cross-sectional layout in Figure 2.

Following the material measurements of the a-SIZO channel material, its electrical characteristics were measured. Figure 3a shows a transfer (I_D-V_G) curve of proposed a-SIZO based FET, exhibiting a clear n-type behavior with maximum mobility of 9.35 cm^2/Vs, a threshold voltage of -0.35 V, and an on/off current ratio in the order of 1×10^6 at V_D of 5V. Additionally, the field-effect mobility was calculated by the following formula, $\mu_{eff} = L\ g_m/W\ C_{ox}V_D$, where the

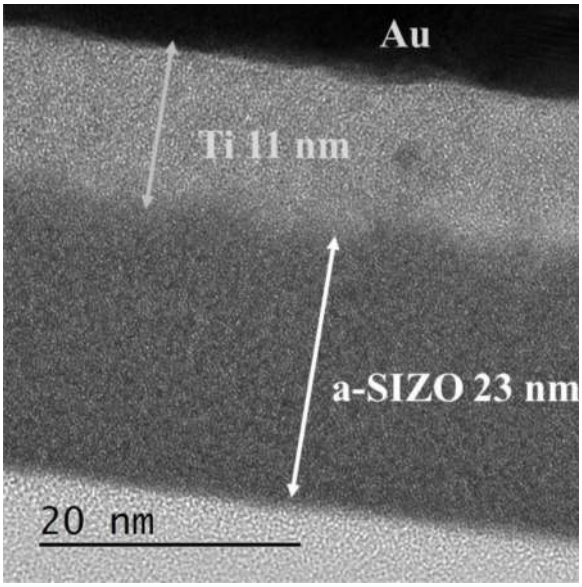

FIGURE 2. Cross-sectional TEM overview of amorphous SIZO channel material.

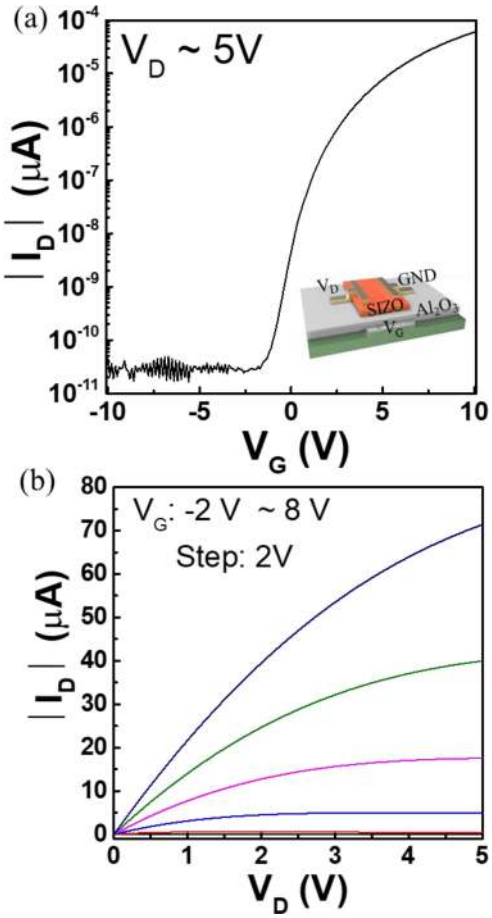

FIGURE 3. Transistor characteristics in terms of (a) transfer and (b) output curves of the proposed FET device, respectively.

channel length (L) and width (W) is defined as 20 μm and 100 μm, respectively. High saturation current at high voltage range and linear behavior at the low voltage range can be

TABLE 1. FET characteristics comparison of proposed a-SIZO FET with previously reported oxide semiconductors.

Oxide Material	Deposition Method	Temperature Process (°C)	Mobility (cm^2/Vs)	On/Off ratio	V_G / V_D (V)	Ref.
a-IZO a-IGZO	Spin Coating	<250	10	10^8	-50 ~ 50 / 5	[12]
ZnO	Spin Coating	500	5.25	10^5	-20 ~ 60 / 50	[13]
a-IGZO	CCP magnetron sputtering	100	26.03	10^7	-20 ~ 20 / 10	[14]
a-IGZO	RF magnetron Sputtering	150	13.40	10^6	-10 ~ 20 / 0.1	[15]
a-SIZO	Rf magnetron Sputtering	<150	9.38	10^6	-10 ~ 10 / 5	This work

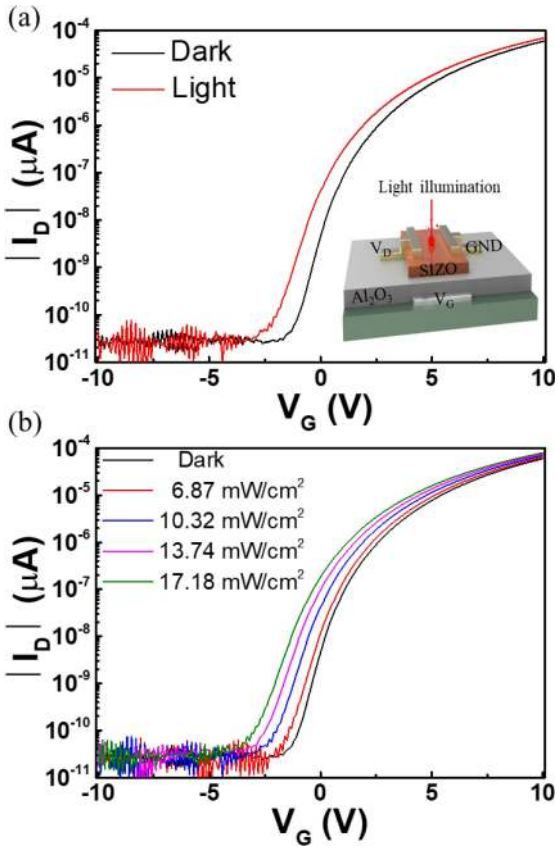

FIGURE 4. Transfer curve under (a) dark/light conditions and (b) various power intensities of red illuminations.

observed in the output curve, shown in Figure 3b, where the gate-bias voltage was applied in the range of -2 V $\sim$ 8 V with an interval -2 V, that attributes an excellent ohmic contact of Ti/Au electrodes based on the proposed channel material. Additionally, the proposed a-SIZO transistor performance is compared by previously reported FETs based on oxide semiconductors with different deposition methods, revealing a stable electrical performance (Table 1).

To analyze the optical properties of the proposed a-SIZO based FET device, the transistor properties were measured under red-light illumination wavelength of 638 nm along with dark conditions, as indicated by the 3D section view in the inset of Figure 4a. Figure 4a shows a comparison of the

transfer ($I_D - V_D$) curve of proposed a-SIZO based phototransistor under light and dark conditions, where the red-light is exposed at power intensity of 10.32 mW/cm^2 and a gradual shift in threshold voltage (V_{Th}) was observed during the experiment. Additionally, exposure to red-light at different power intensities (6.87 mW/cm^2 to 17.18 mW/cm^2) yields a higher photogeneration current due to wide bandgap of around 3.0 eV where the photogenerated photons penetrate into the bandgap the excites electrons, so the current (I_D) increases with V_{TH} shift, as shown in Figure 4b. The optical results obtained from the presented a-SIZO phototransistor were then compared with recently reported phototransistors based on oxide semiconductors materials, where the photoresponse was obtained by different doping methods (Table 2). Due to the effect of Si concentrations in a-SIZO semiconductor, the bandgap can vary and photogeneration current can obtain without any dopant [16].

To analyze the photo-responsive behavior of proposed a-SIZO based phototransistor, the threshold voltage shift (ΔV_{Th}) and photocurrent (I_{photo}) were measured under different power intensities of red-light ranges, as shown in Figures 5a and 5b, respectively. The optical results show high uniformity and stability of the photodetection performance of the proposed a-SIZO based phototransistor. Then, the significant key figure of merit for photodetection, the time response behavior of the proposed device was measured under red-light illumination with a power intensity of 10.32 mW/cm^2. The rise time of 0.9 s and fall time of 2.02 s were observed with high stability, describing the robustness of the proposed phototransistor, shown in Figure 5c.

To analyze the key figure of merit for photodetection, the responsivity, detectivity, sensitivity, and gain parameters were measured under different power levels. The photoresponsivity (R) was obtained in the range of 15.23 A/W $\sim$ 7.023 A/W at different incident light power levels (6.87 mW/cm^2 $\sim$ 17.18 mW/cm^2), calculated by $R = I_{photo}/P_{inc}$ (A/W), where P_{inc} represents the incident power and I_{photo} represents the total current at a specific power, shown in Figure 6a. Photocurrent, here, was obtained by $I_{photo} = I_{total} - I_{dark}$, where I_{total} represents the total current measured at a specific power and I_{dark} represents the current at dark conditions. Then, the specific detectivity (D*) was measured at various incident light power scales and the results show a linear trend in the range of 12-4.5$\times 10^{12}$ jones for detectivity as shown in Figure 6b. Here, the specific detectivity is calculated by $D^* = RA^{1/2}/(2eI_{dark})^{1/2}$, where A defines the illuminated area, and e defines the elementary charge value. Next, the sensitivity was measured, and the consequences show linear and stable response under various incident light power levels (Figure 6c). The photo-gain (G) of proposed a-SIZO phototransistor at different incident power scales was calculated by $G = I_{photo}/(e\times\Delta n\times A)$, where Δn defines the carrier concentration of the photoinduced trapped electrons [21] and the results show a gain is up to 10^5 (Figure 6d). The carrier concentration was obtained by the formula $\Delta n = C_g\times\Delta V_{TH}/e$, where C_g represents the gate capacitance of 1.6×10^{-7} F/cm^2 and ΔV_{TH} represents the voltage shift at specific light incident power. In this regard, the results show that the photodetection behavior of the proposed a-SIZO based phototransistor exhibits highly sensitive and responsive performance.

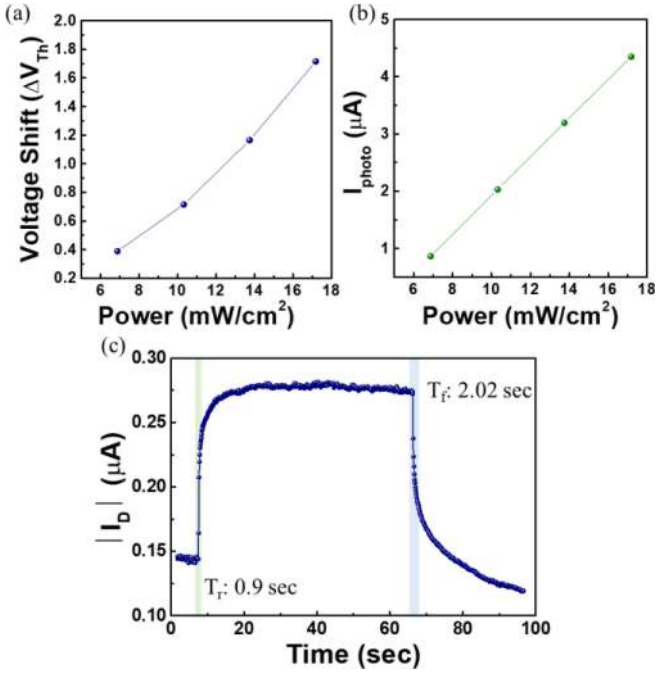

FIGURE 5. The photo-responsive behavior in terms of (a) ΔV_{Th}, (b) I_{photo}, and (c) time-domain.

TABLE 2. Comparison of photo-responsive behavior with previously reported oxide semiconductors.

Oxide Material	Combining Material	Responsivity (A/W)	Rise time (s)	Fall time (s)	Ref.
a-IGZO	Graphene dots	5	N.A	N.A	[17]
a-IGZO	$MAPbI_3$	0.025	0.04	0.1	[18]
a-IGZO	MoS_2	0.055	2.6	1.7	[19]
ZnO	Quantum dots	0.032 (mA / W ~ red light)	N.A	N.A	[20]
a-SIZO	None	15.23	0.9	2.02	This work

The enhancement-load type unipolar inverter based on n-type semiconductor material is generally designed in a way that connects the drain electrode directly to the gate electrode of load FET which fixes the current level depending on drain voltage (V_{DD}) [22], [23]. The real image of the fabricated a-SIZO based inverter can be visualized in Figures 7a. Figure 7b shows the voltage transfer and inverter gain curves of presented enhancement-load type inverter based on a-SIZO channel material at $V_{DD} \sim 1$V. The represented unipolar inverter devices show a maximum voltage gain

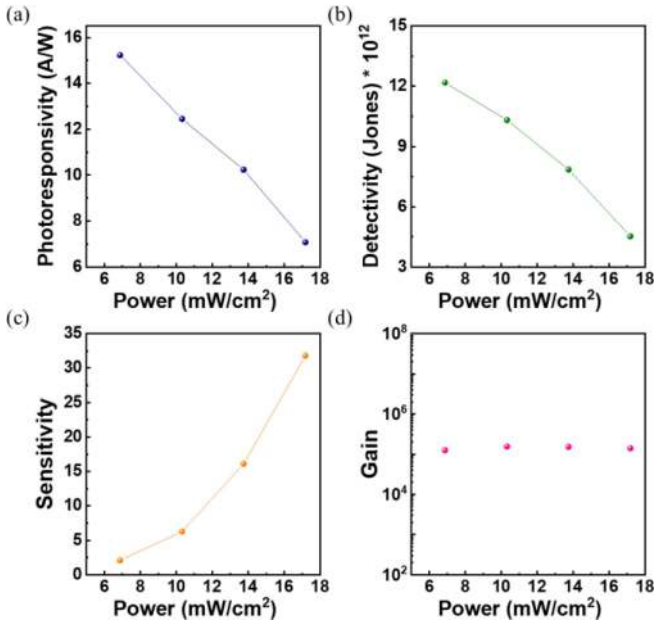

FIGURE 6. The key figure of merit for photodetection parameters in terms of (a) photoresponsivity, (b) detectivity, (c) sensitivity, and (d) gain.

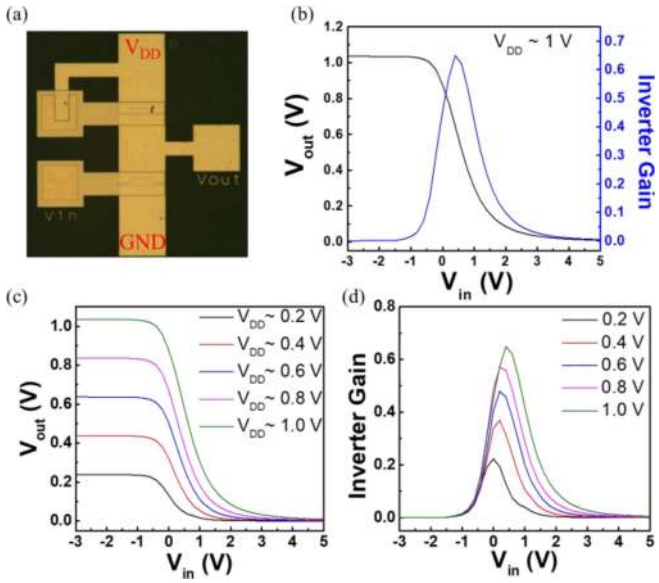

FIGURE 7. (a) A real image of the proposed inverter device. (b) The inverting curve of the device with inverter gain. (c, d) Inverting and gain characteristics at different V_{DD}.

of 0.645 at VDD ∼ 1V. The inverter gain (I_G) is calculated by the following formula: I_G = abs. (dV_{OUT}/dV_{IN}), where V_{OUT} represents the output voltage and V_{IN} represents the input voltage of the proposed inverter device. Additionally, the voltage transfer properties and inverter gain of proposed inverter devices were analyzed under various V_{DD} values ranges from 1 V to 0.2 V, elaborating a tendency of inverter characteristics depending on different V_{DD}, shown in Figures 7c and 7d, respectively.

Next, the time-domain behavior of the proposed inverter device was characterized at constant V_{DD} pulse of 1 V and

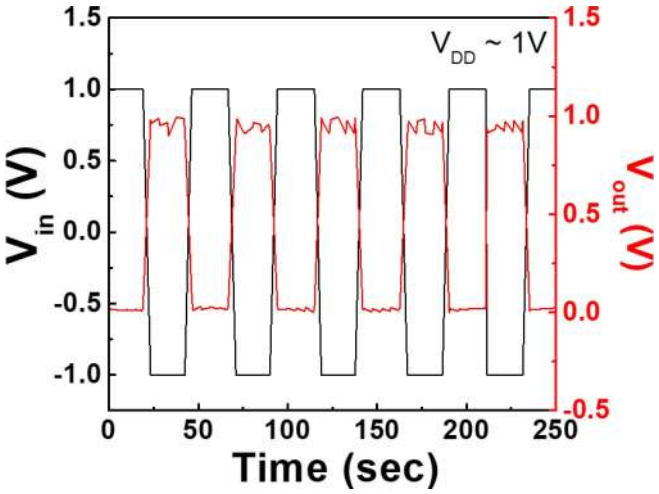

FIGURE 8. Time-domain characteristics for a pulsed input voltage from −1 V to 1 V.

TABLE 3. Comparison of proposed a-SIZO based inverter device with previously reported oxide semiconductor along with photo measurement system.

Semiconductor Material	Inverter - type Structure	V_{DD}	Gain	Photo-response Measurements	Ref.
a-IGZO	Depletion-load (Enhancement-load)	20	-20.5 (V/V) (-1.5 (V/V))	N.A	[22]
SIZO	Depletion-load	3	9.8	Photo-stressing	[7]
AuNps/P3HT	Depletion-load (Enhancement-load)	40 (40)	6.5 (No gain)	N.A	[24]
ZTO	Enhancement-load	5	1	N.A	[25]
a-SIZO	Enhancement-load	1	0.645	Photo-inducing	This work

0 V up to 250 s with an interval of 25 s, demonstrating a stable and reliable switching throughout the measurements, shown in Figure 8.

The optoelectronic behavior of the proposed enhancement-load type unipolar inverter device was then examined under different red-light illumination intensities (6.87 mW/cm^2 to 17.18 mW/cm^2). Figure 9a shows a 3D section view of the proposed unipolar inverter device. A gradual shift in voltage and increase in inverter gain were observed when exposed to red-light illumination under different power intensities ranges from 6.87 mW/cm^2 to 17.18 mW/cm^2, as shown in Figures 9b and 9c, respectively, revealing a stable and linear photo-responsive behavior. In addition, the proposed enhancement-load type unipolar inverter device properties were compared by previous reported unipolar inverter devices in terms of inverter type, applied V_{DD}, gain, and possible photo-measurements (Table 3), revealing an excellent photo-inducing property.

Additionally, further evaluate the key figures of merit for photodetection of the proposed photoinduced inverter device, the voltage shift difference (ΔV), inverter gain shift, and time

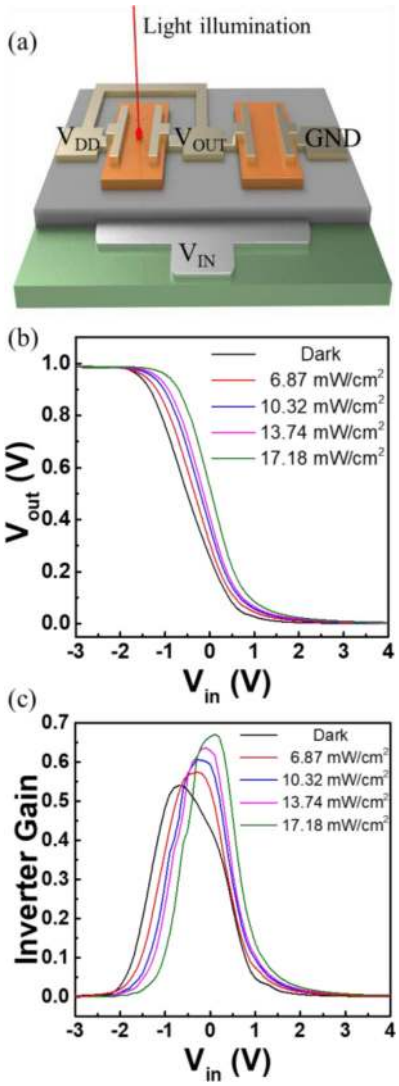

FIGURE 9. **(a) A schematic layout of the proposed inverter device under light illumination. (b) Inverting and (c) gain characteristics under different power intensities of red-light.**

response were then analyzed. The voltage shift difference (ΔV) was calculated by $\Delta V = V_{dark} - V_{light}$, where V_{dark} represents the voltage drop measured at the dark condition and V_{light} represents the voltage drop measured at different power intensities of red-light illuminations. Figures 10a and 10b show an excellent linear and stable behavior of the photoinduced inverter device in terms of voltage shift difference and inverter gain at different power levels ranges from 6.87 mW/cm^2 to 17.18 mW/cm^2. In Figure 10b, the inverter gain shift (IGS) was calculated by $IGS = G_{photo} - G_{dark}$, where G_{photo} represents the inverter gain at specific incident light power and G_{dark} represents the inverter gain at dark condition. The results show highly sensitive photodetection using integrated circuits (inverter device).

Then, the time-domain behavior of the proposed photoinduced inverter device was analyzed where V_{IN} (0.5 V) and V_{DD} (0.6 V) were fixed. The V_{OUT} was measured under a pulse of red-light illumination power intensity of

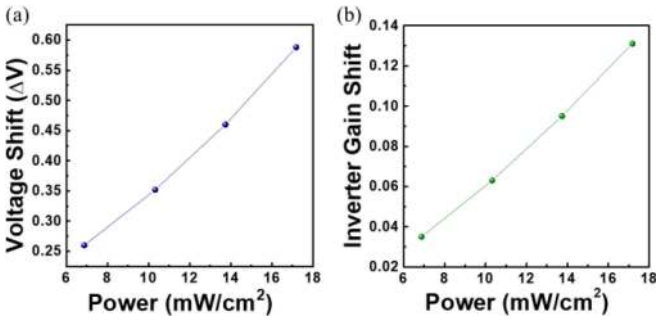

FIGURE 10. **The photo-responsive behavior of the proposed inverter device in terms of (a) ΔV and (b) inverter gain shift.**

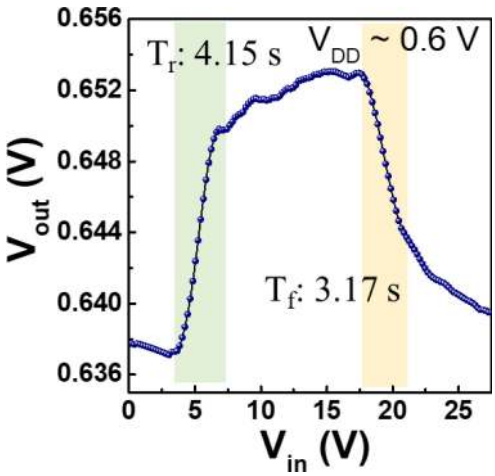

FIGURE 11. **Time-domain characteristics of the proposed photo-induced inverter device when exposed to red light with a power of 10.32 mW/cm^2.**

10.32 mW/cm^2, demonstrating a gradual increase in V_{OUT} with a rise time of 4.15 s and falling time of 3.17 s, as shown in Figure 11. The results show a highly sensitive and responsive performance of photodetection in the presented photoinduced inverter device, promising great potential for futuristic application in the field of integrated electronics.

IV. CONCLUSION

In this work, an enhancement-load type inverter device with a-SIZO unipolar channel material was produced via low-temperature processing and analyzed. The a-SIZO based FET showed stable electrical and optical performance with maximum mobility of 9.8 cm^2/Vs, high on/off ratio of $\sim 10^6$, and linear photo-responsive behavior. The proposed inverter device exhibited a high inverter gain of 0.7 at V_{DD} of 1 V, and linear voltage shift and inverter gain under the varying intensity of red-light illumination (80 to 200 μW), and hence provides a unique platform for future integrated electronic applications.

ACKNOWLEDGMENT

The authors thank K.-S. Cho and S. Park in Samsung Advanced Institute of Technology for TEM measurements and analysis.

REFERENCES

[1] E. Fortunato, P. Barquinha, and R. Martins, "Oxide semiconductor thin-film transistors: A review of recent advances," *Adv. Mater.*, vol. 24, no. 22, pp. 2945–2986, 2012, doi: 10.1002/adma.201103228.

[2] K. Nomura, H. Ohta, A. Takagi, T. Kamiya, M. Hirano, and H. Hosono, "Room-temperature fabrication of transparent flexible thin-film transistors using amorphous oxide semiconductors," *Nature*, vol. 432, no. 7016, p. 488–492, Nov. 2004, doi: 10.1038/nature03090.

[3] J. H. Na, M. Kitamura, and Y. Arakawa, "Organic/inorganic hybrid complementary circuits based on pentacene and amorphous indium gallium zinc oxide transistors," *Appl. Phys. Lett.*, vol. 93, no. 21, pp. 1–4, 2008, doi: 10.1063/1.3039779.

[4] A. Dodabalapur, J. Baumbach, K. Baldwin, and H. E. Katz, "Hybrid organic/inorganic complementary circuits," *Appl. Phys. Lett.* vol. 68, no. 16, pp. 2246–2248, Apr. 1996, doi: 10.1063/1.115873.

[5] K. Myny, "The development of flexible integrated circuits based on thin-film transistors," *Nat. Electron.*, vol. 1, no. 1, pp. 30–39, 2018, doi: 10.1038/s41928-017-0008-6.

[6] J. Wang, Y. Li, Y. Yang, and T.-L. Ren, "Low-voltage unipolar inverter based on top-gate electric-double-layer thin-film transistors gated by silica proton conductor," *IEEE Electron Device Lett.*, vol. 38, no. 7, pp. 875–878, Jul. 2017, doi: 10.1109/LED.2017.2700293.

[7] B. H. Lee, S. Kim, and S. Y. Lee, "Investigation on dependency mechanism of inverter voltage gain on current level of photo stressed depletion mode thin-film transistors," *Solid-State Electron.*, vol. 156, pp. 5–11, Jun. 2019, doi: 10.1016/j.sse.2019.03.030.

[8] T. Iwasaki, N. Itagaki, T. Den, and H. Kumomi, "Combinatorial approach to thin-film transistors using multicomponent semiconductor channels: An application to amorphous oxide semiconductors in In-Ga-Zn-O system," *Appl. Phys. Lett.*, vol. 90, no. 24, pp. 1–4, 2007, doi: 10.1063/1.2749177.

[9] G. Han, S. Cao, Q. Yang, W. Yang, T. Guo, and H. Chen, "High-performance all-solution-processed flexible photodetector arrays based on ultrashort channel amorphous oxide semiconductor transistors," *ACS Appl. Mater. Interfaces*, vol. 10, no. 47, pp. 40631–40640, 2018, doi: 10.1021/acsami.8b14143.

[10] J. Bae, I. Jeong, and S. Lee, "Wavelength-dependent optical instability mechanisms and decay kinetics in amorphous oxide thin-film devices," *Sci. Rep.*, vol. 9, no. 1, pp. 1–6, 2019, doi: 10.1038/s41598-019-39744-8.

[11] W. Yu *et al.*, "High-performance calcium-doped zinc oxide thin-film transistors fabricated on glass at low temperature," *Jpn. J. Appl. Phys.*, vol. 55, no. 4S, 2016, Art. no. 04EK05, doi: 10.7567/JJAP.55.04EK05.

[12] K. K. Banger *et al.*, "Low-temperature, high-performance solution-processed metal oxide thin-film transistors formed by a 'sol–gel on chip' process," *Nat. Mater.*, vol. 10, no. 1, pp. 45–50, 2011, doi: 10.1038/nmat2914.

[13] B. S. Ong, C. Li, Y. Li, Y. Wu, and R. Loutfy, "Stable, solution-processed, high-mobility ZnO thin-film transistors," *J. Amer. Chem. Soc.*, vol. 129, no. 10, pp. 2750–2751, 2007, doi: 10.1021/ja068876e.

[14] C. Liu, Y. Sun, H. Qin, Y. Liu, S. Wei, and Y. Zhao, "Low-temperature, high-performance InGaZnO thin-film transistors fabricated by capacitive coupled plasma-assistant magnetron sputtering," *IEEE Electron Device Lett.*, vol. 40, no. 3, pp. 415–418, Mar. 2019, doi: 10.1109/LED.2019.2896111.

[15] D. Koretomo, S. Hamada, M. Mori, Y. Magari, and M. Furuta, "Marked improvement in reliability of 150°C processed IGZO thin-film transistors by applying hydrogenated IGZO as a channel material," *Appl. Phys. Exp.*, vol. 13, no. 7, 2020, Art. no. 076501, [Online]. Available: https://www.x-mol.com/paperRedirect/1268991910220427264.

[16] J. Y. Choi *et al.*, "Effect of Si on the energy band gap modulation and performance of silicon indium zinc oxide thin-film transistors," *Sci. Rep.*, vol. 7, no. 1, pp. 1–8, 2017, doi: 10.1038/s41598-017-15331-7.

[17] Z. Pei, H.-C. Lai, J.-Y. Wang, W.-H. Chiang, and C.-H. Chen, "High-responsivity and high-sensitivity graphene dots/a-IGZO thin-film phototransistor," *IEEE Electron Device Lett.*, vol. 36, no. 1, pp. 44–46, Jan. 2015, doi: 10.1109/LED.2014.2368773.

[18] S. Du *et al.*, "Oxide semiconductor phototransistor with organolead trihalide perovskite light absorber," *Adv. Electron. Mater.*, vol. 3, no. 4, 2017, Art. no. 1600325, doi: 10.1002/aelm.201600325.

[19] J. Yang *et al.*, "MoS2–InGaZnO heterojunction phototransistors with broad spectral responsivity," *ACS Appl. Mater. Interfaces*, vol. 8, no. 13, pp. 8576–8582, 2016, doi: 10.1021/acsami.5b11709.

[20] J. Yu, B. J. Kim, S. Park, I. K. Han, and S. J. Kang, "Red/green/blue selective phototransistors with a hybrid structure of quantum-dots and an oxide semiconductor," *Jpn. J. Appl. Phys.*, vol. 57, no. 4, 2018, Art. no. 044001, doi: 10.7567/JJAP.57.044001.

[21] W. Zhang *et al.*, "Ultrahigh-gain photodetectors based on atomically thin graphene-MoS_2 heterostructures," *Sci. Rep.*, vol. 4, p. 3826, Jan. 2014, doi: 10.1038/srep03826.

[22] J. H. Ryu, G.-W. Baek, S. J. Yu, S. G. Seo, and S. H. Jin, "Photosensitive full-swing multi-layer MoS_2 inverters with light shielding layers," *IEEE Electron Device Lett.*, vol. 38, no. 1, pp. 67–70, Jan. 2017, doi: 10.1109/LED.2016.2633479.

[23] X. Huang *et al.*, "Large-swing a-IGZO inverter with a depletion load induced by laser annealing," *IEEE Electron Device Lett.*, vol. 35, no. 10, pp. 1034–1036, Oct. 2014, doi: 10.1109/LED.2014.2345412.

[24] S.-T. Han, Y. Zhou, Z.-X. Xu, and V. A. L. Roy, "Controllable threshold voltage shifts of polymer transistors and inverters by utilizing gold nanoparticles," *Appl. Phys. Lett.*, vol. 101, no. 3, 2012, Art. no. 033306, doi: 10.1063/1.4737422.

[25] C. Fernandes *et al.*, "A sustainable approach to flexible electronics with zinc-tin oxide thin-film transistors," *Adv. Electron. Mater.*, vol. 4, no. 7, 2018, Art. no. 1800032, doi: 10.1002/aelm.201800032.